Fig. S1. Proliferation curves of *Dictyostelium* strains under growth conditions.

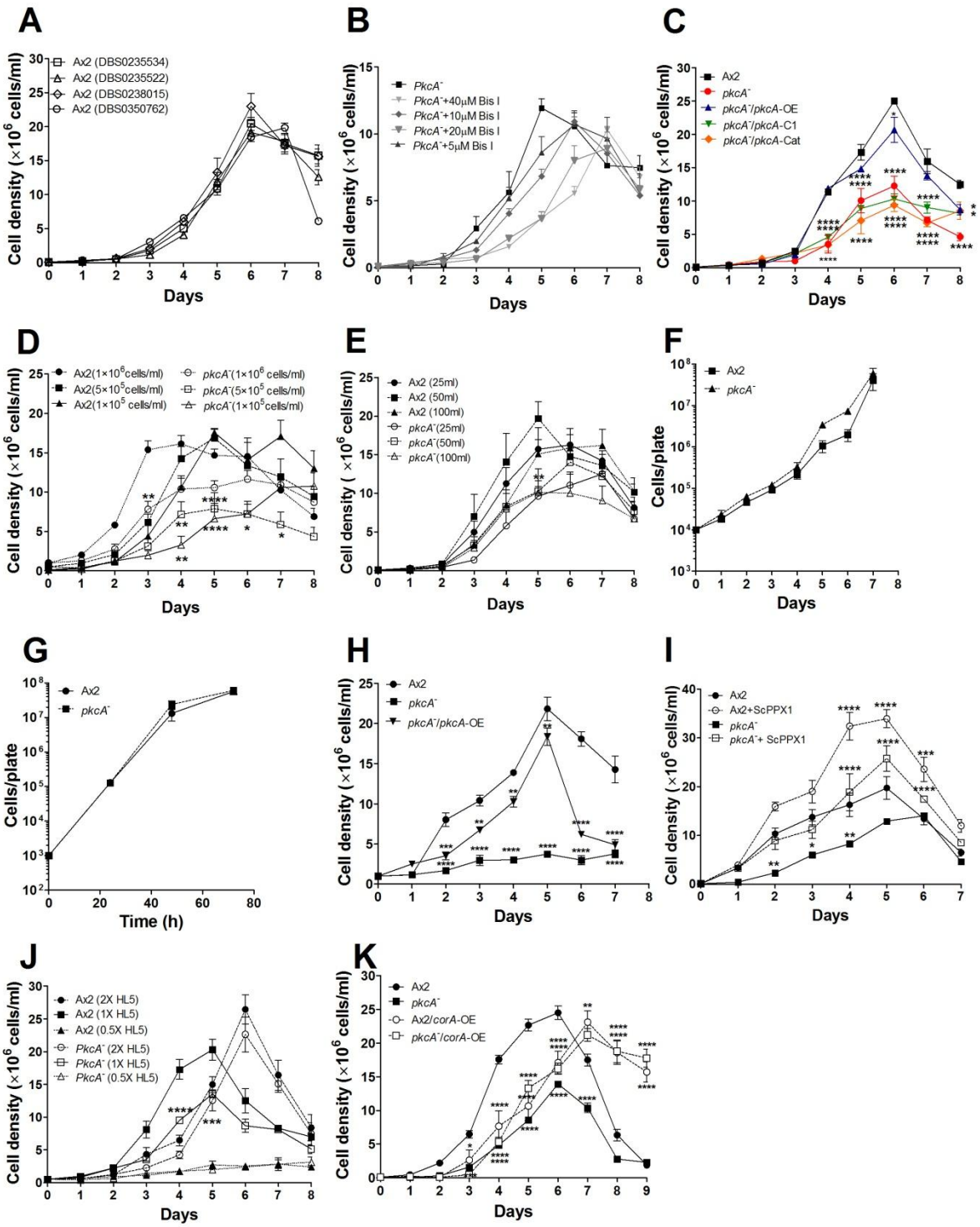

Fig. S1. Proliferation curves of *Dictyostelium* strains under growth conditions. (A) Proliferation assays of all the parental Ax2 strains used to generate various mutants used in the study. SP densities (in units of 10^6 cells/ml) were 21.3±0.4 for Ax2 (DBS0235534), 23.0±1.9 for Ax2 (DBS0238015), 19.9±0.8 for Ax2 (DBS0235522) and 20.4±0.7 for Ax2 (DBS0350762). (B) *PkcA*$^-$ cells were treated with different concentrations of Bis I at an interval of 24 h, and the proliferation assays were then carried out. The density at which cells enter SP was dependent on the Bis I dose ((10 μM ($p<0.05$), 20 μM ($p<0.01$) and 40 μM ($p<0.001$)(one- way ANOVA with Tukey's multiple comparisons)). (C) To determine the particular domain of pkcA that is important for cell proliferation and SP entry, *pkcA*$^-$ cells were independently transformed with the regulatory C1 (*pkcA*$^-$/act15::*pkcA*-C1domain) and the catalytic kinase domain (*pkcA*$^-$ /act15::*pkcA*-cat domain) and a proliferation assay with a starting density of 1×10^5 cells/ml was performed. The cell number was determined every day using a hemocytometer. SP cell density is included in Table S1. (D) Cells were inoculated at the indicated initial densities and proliferation assays were performed. The proliferation kinetics of *pkcA*$^-$ cells inoculated at 1×10^5, 5×10^5 and 1×10^6 cells/ml were compared to Ax2 cells at the respective density. (E) To check if differences in aeration affect cell proliferation, Ax2 and *pkcA*$^-$ cells were cultured in three different sized flasks (25, 50 and 100 ml with 10 ml media in each) and the cell density was determined using a hemocytometer every day. The proliferation curves of *pkcA*$^-$ cells grown in 25, 50 and 100 ml flasks were compared to those of Ax2 grown in 25, 50 and 100 ml flasks respectively. (F) Proliferation assay in Petri dishes. (G) Cells were mixed with bacteria and spread on SM/5plates and the cell numbers were counted at the indicated time points. (H) Cells were inoculated at a density of 1×10^6 cells/ml in FM minimal media and cell density was measured every day. (I) Ax2 and *pkcA*$^-$ cells were treated with 0.15μg/ml ScPPX1 or buffer and a proliferation assay was performed. (J) Proliferation assay was performed in 2X and 0.5X along with 1X HL5 and the cell density was measured every day. The proliferation curves of *pkcA*$^-$ cells grown in 2X, 1X and

0.5X HL5 were compared to those of Ax2 grown in 2X, 1X and 0.5X HL5 respectively. (K) Proliferation assay of Ax2 and *pkcA*$^{-}$ cells overexpressing Coronin A. The growth curve of *pkcA*$^{-}$/*CorA*-OE cells was similar to Ax2/*CorA*-OE. All values are mean ± SEM; n=3 independent experiments and were analyzed using two-way ANOVA with Bonferroni's multiple comparisons for all the graphs. ****p<0.0001,***p<0.001,**p<0.01, *p<0.05. and ns-not significant.

Fig. S2. CM treatments.

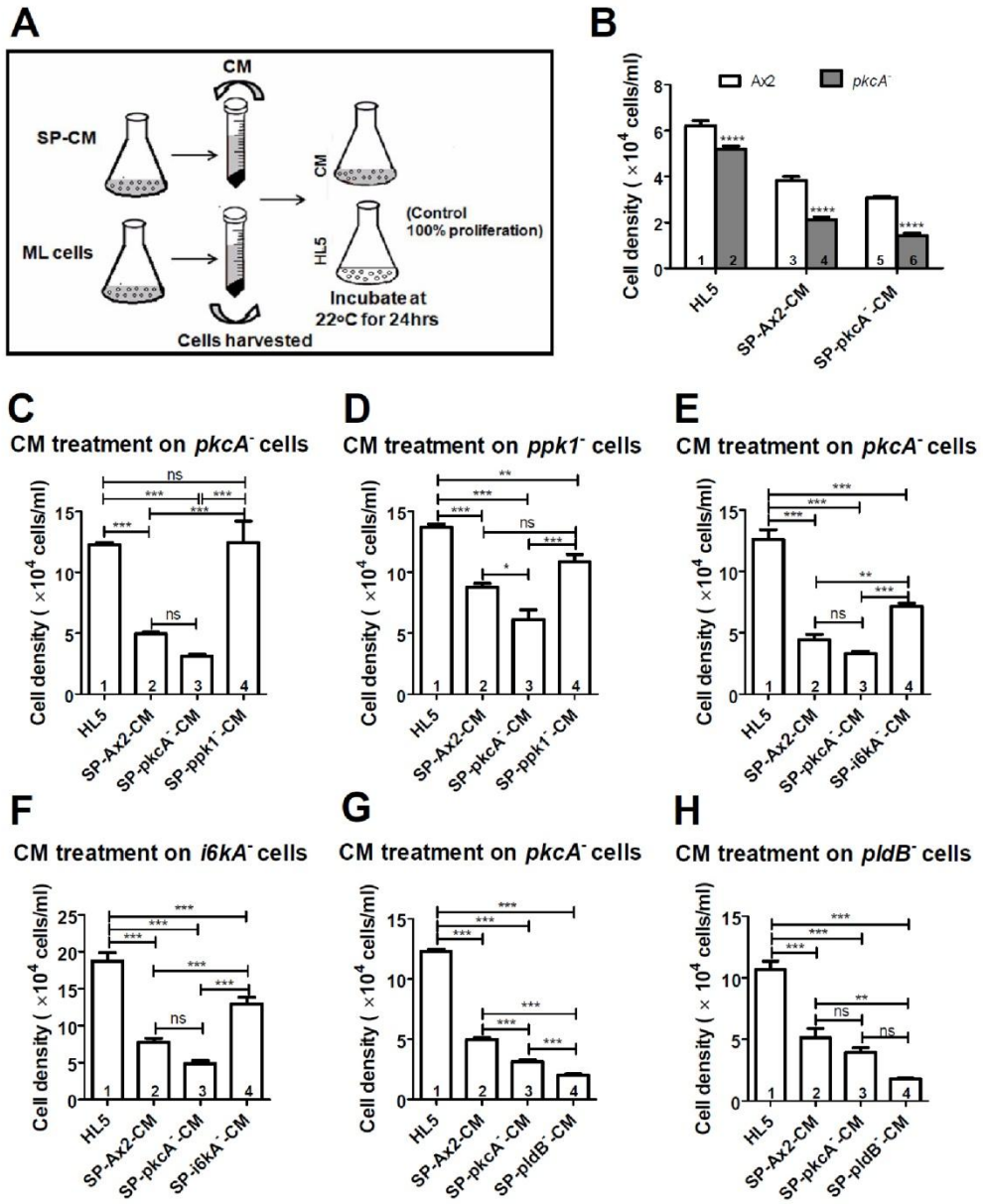

Fig. S2. CM treatments. (A) Schematic representation of the experimental design to study the effect of CM on proliferation in shaking conditions. (B) Ax2 and *pkcA*$^-$ cells were treated with their respective SP-CM from shaking cultures, incubated at 22°C for 24 h with constant shaking (150 rpm) and after 24 h the cells were counted using a hemocytometer. Bar 1 and 2: Control. Ax2 and *pkcA*$^-$ cells grown in HL5 while testing SP-CM; bar 3 and 4: CM was collected from Ax2 cultures after they reached the maximum cell density (SP density; 20-25x10^6 cells/ml). This CM was tested on Ax2 and *pkcA*$^-$ cells; bar 5 and 6: CM was collected from *pkcA*$^-$ cultures after

they reached the maximum cell density (SP density; 10-15x10^6 cells/ml). This CM was tested on Ax2 and *pkcA*$^-$ cells. (C) To know whether the CM with reduced polyP can rescue *pkcA*$^-$ proliferation, *pkcA*$^-$ cells were treated with SP-CM from SP-*ppk1*$^-$-CM. (E) *PkcA*$^-$ cells were treated with SP-*i6kA*$^-$-CM to check if the proliferation defect can be rescued. (G) Addition of SP-*pldB*$^-$-CM to *pkcA*$^-$ to determine the extent to which proliferation is inhibited. (D, F and H) Addition of SP-*pkcA*$^-$-CM to *ppk1*$^-$ (D), *i6kA*$^-$ (F) and *pldB*$^-$ (H) to know the extent to which proliferation is inhibited. The testing was done on *pkcA*$^-$ cells (C, E and G), *ppk1*$^-$ (D), *i6kA*$^-$ (F) and *pldB*$^-$ (H). Bar 1: Control: *pkcA*$^-$ (C, E and G), *ppk1*$^-$ (D), *i6kA*$^-$ (F) and *pldB*$^-$ (H) cells grown in HL5; bar 2: CM was collected from Ax2 cultures after SP density was reached. bar 3: CM was collected from *pkcA*$^-$ cultures after they reached the maximum cell density. bar 4: CM was collected from *ppk1*$^-$(C and D), *i6kA*$^-$ (E and F) and *pldB*$^-$(G and H) cultures after they reached the maximum cell density. Data are means ± SEM from n=3 biologically independent samples. Statistical significance was assessed by two-way ANOVA with Bonferroni's multiple comparisons (B) and one-way ANOVA with Tukey's multiple comparisons (C-H). . ***p<0.001, **p<0.01and *p<0.05.

Fig. S3. The secreted factors AprA and CfaD are not responsible for the growth defect in *pkcA*⁻ cells.

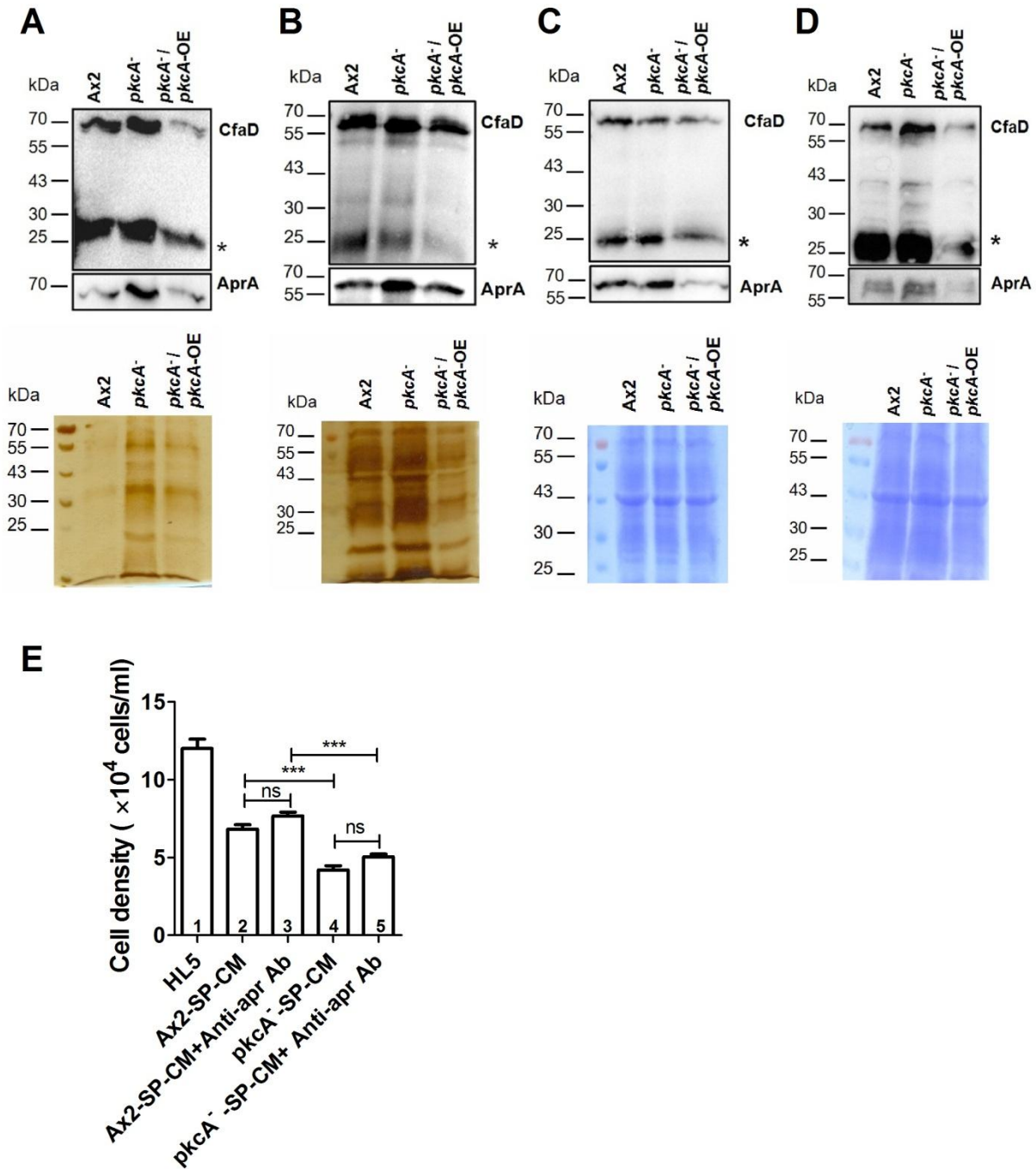

Fig. S3. The secreted factors AprA and CfaD are not responsible for the growth defect in *pkcA*⁻ cells. (A and B) To check if the levels of these two autocrine factors were abnormal in *pkcA*⁻, ML-CM (A) and SP-CM (B) from Ax2, *pkcA*⁻ and *pkcA*⁻/*pkcA*-OE were collected and the extracellular levels of AprA and CfaD were examined by western blotting. Note that total protein

levels are high in *pkcA*$^{-}$ cells in both ML and SP CM. Images are representative of three independent experiments. (C and D) ML (C) and SP (D) cells were collected and the intracellular levels of AprA and CfaD were examined by western blotting. (E) To ascertain if the inhibitory activity of SP-*pkcA*$^{-}$-CM is due to excess AprA, the CM was treated with anti-AprA antibody (1:150) and thereafter, cell proliferation was examined in Ax2 and *pkcA*$^{-}$ cells. Surprisingly, there was no difference in the proliferation rates in both cell types suggesting that high aprA levels in ML- *pkcA*$^{-}$-CM do not contribute to the defective growth of the mutant. The CMs were tested on Ax2 cells. Bar 1: Control. Ax2 cells grown in HL5 while testing SP-CM; bar 2 and 4: CM was collected from Ax2 and *pkcA*$^{-}$ culture after they reached the maximum cell density. bar 3 and 5: CM was collected from Ax2 and *pkcA*$^{-}$ cultures after they reached the maximum cell density. This CM was treated with anti-AprA antibody. Data are means ± SEM; n≥3 biologically independent experiments. Statistical significance was assessed by one-way ANOVA with Tukey's multiple comparisons. ***p<0.0001 and ns-not significant.

Fig. S4: Extensive variation of extracellular polyP levels in pinocytosis mutants.

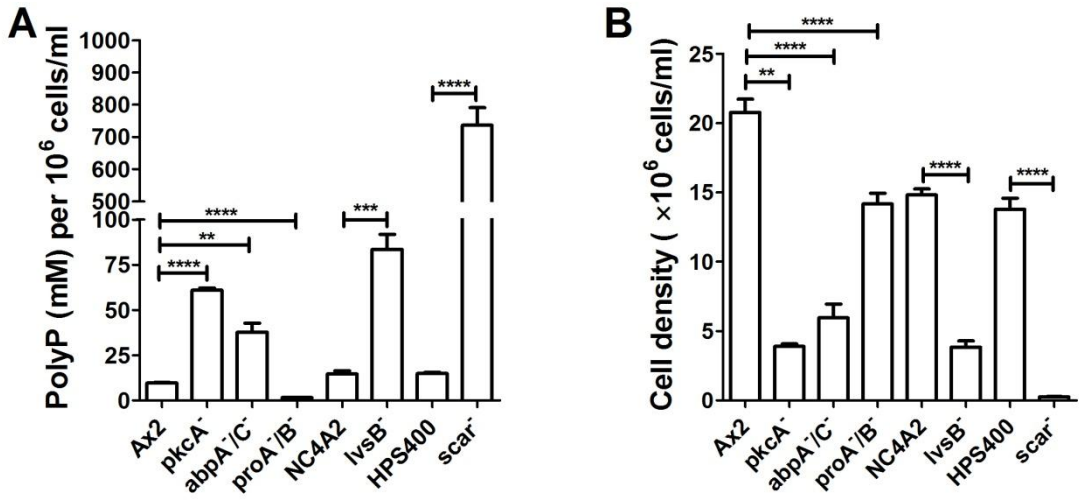

Fig. S4. Extensive variation of extracellular polyP levels in pinocytosis mutants. (A) Mutants and parental strains were grown in FM media and the stationary phase cell densities were recorded. (B) Extracellular CM from the cells were collected at the SP cell density, polyP concentration was estimated and normalized to respective SP cell density. All data represents means ± SEM from n=3 independent experiments. For each strain, the data was analyzed using two-tailed paired *t*-test and compared to parental strains. The polyP levels and SP densities of *pkcA*$^-$, *abpA*$^-$*/C*$^-$ and *proA*$^-$*/B*$^-$ were compared to those of Ax2 (Ax2-214 (DBS0235534); *lvsB*$^-$ to NC4A2 and *scarA*$^-$ to HPS400. **** p<0.0001, *** p<0.001 and ** p < 0.01.

Fig. S5. Cell cycle analysis of *pkcA*⁻ cells suggest large fraction to be multinucleate in shaking conditions.

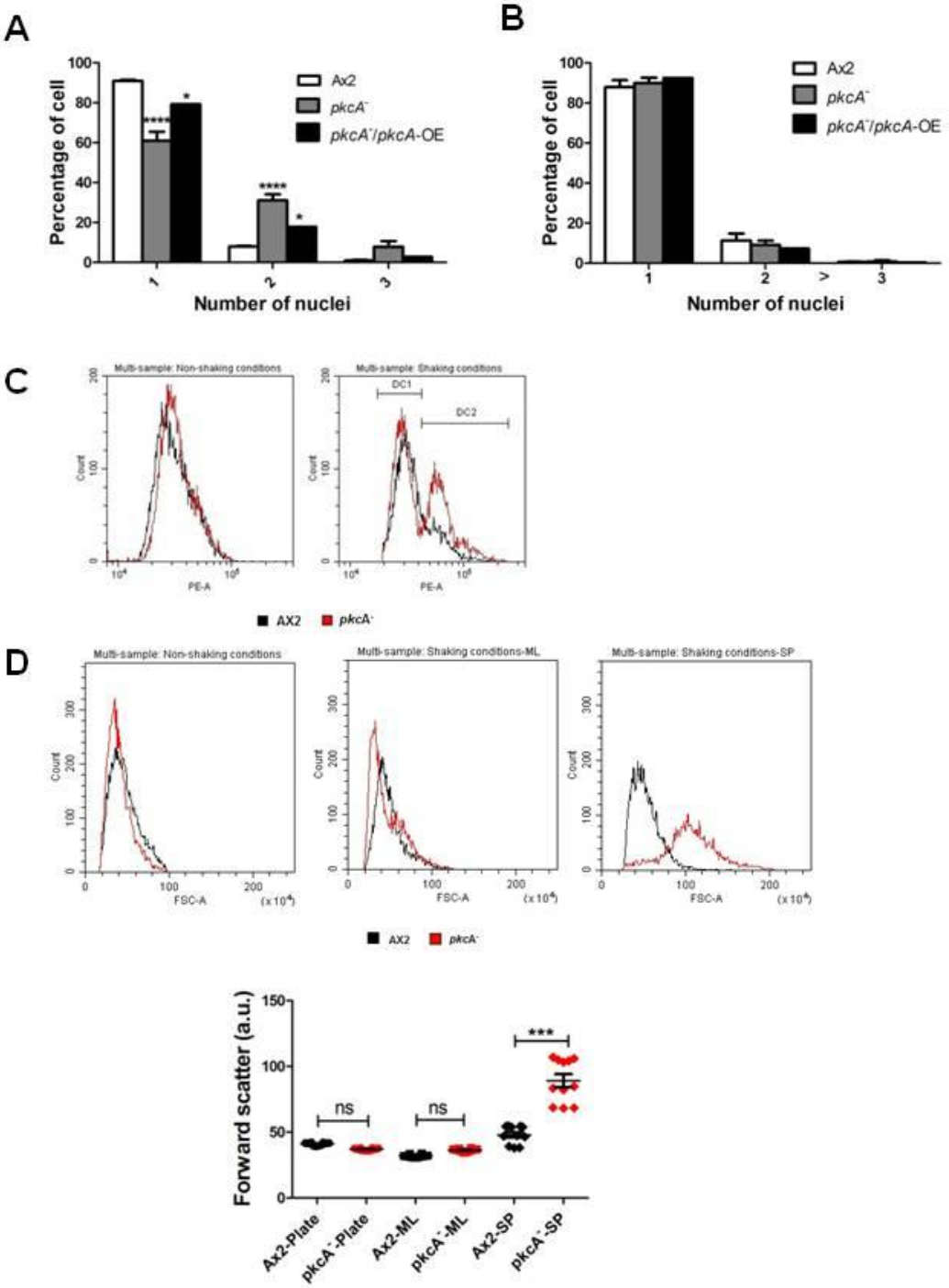

Fig. S5. Cell cycle analysis of *pkcA*$^-$ cells suggests a large fraction are multinucleate in shaking conditions. (A, B) Nuclear content of cells grown in shaking conditions (A) and Petri dishes (B), at least 100 cells were analyzed per experiment; n=3. (C) Cell cycle analysis was carried out using a flow cytometer (CytoFLEX apparatus, Beckman-Coulter, USA) with propidium iodide stained Ax2 and *pkcA*$^-$ cells grown in shaking and non-shaking conditions. The cell cycle phases of both Ax2 and *pkcA*$^-$ cells were almost identical except that in the G2 phase of *pkcA*$^-$ cells, there were two peaks, indicating a fraction of multinuclear cells. (D) Forward scatter of Ax2 and *pkcA*$^-$ cells grown in shaking and non-shaking conditions. For flow cytometry, 10,000 events per experiment were considered. All data represents means ± SEM from n=3 independent experiments and analyzed using two-way ANOVA with Bonferroni's multiple comparisons (A and B) and one-way ANOVA with Tukey's multiple comparisons (D). ****p0.0001, ***p<0.001, *p0.05 and ns- not significant.

Fig. S6: Early stationary phase entry in *pkcA*⁻ cells are not due to myosin II defects.

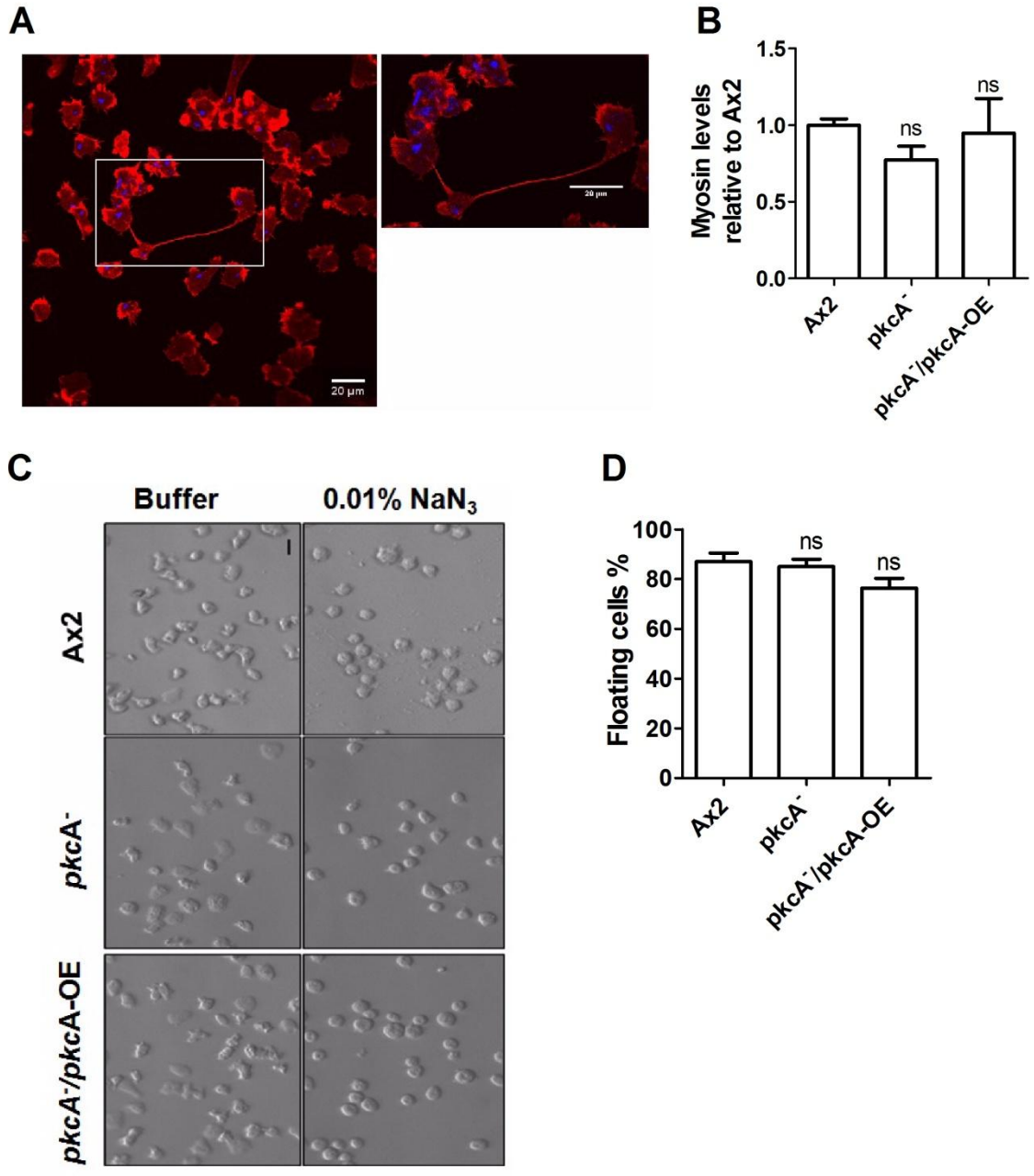

Fig. S6. Early stationary phase entry in *pkcA*⁻ cells are not due to myosin II defects. (A) Similar to *pkcA*⁻, *Dictyostelium* mutants defective in myosin II assembly also show SP entry at a reduced cell density and such impaired growth was not reported when grown in plates (Wang et al., 2011). The multinucleated *pkcA*⁻ cells grown in shaking conditions when transferred to a glass surface go through traction-mediated cytofission like myosin II defective mutants. A

representative image is shown. (B) To examine if the *pkcA*$^-$ growth defects were associated with a myosin II defect, assembled myosin levels were measured in the cytoskeletal fraction of ML cells grown in suspension and normalized to total protein levels. There was no significant difference in the myosin II levels of *pkcA*$^-$ and Ax2 cells. (C and D) Myosin II activity was examined after treating ML *pkcA*$^-$ and Ax2 cells with 0.01% sodium azide for 30 min and the fraction of floating versus adhered cells was counted. Surprisingly, there was no significant difference in the fraction of floating versus adhered cells in Ax2 and *pkcA*$^-$ cells. These results suggesting that myosin II assembly or its function do not contribute to the growth defect of *pkcA*$^-$. Data are means ± SEM; n≥3 biologically independent experiments. Statistical significance was assessed by one-way ANOVA with Tukey's multiple comparisons (B and D). ns-not significant.

Fig. S7. PkcA-GFP localization in lysosomal vesicles and PkcA regulates lysosome dependent processes.

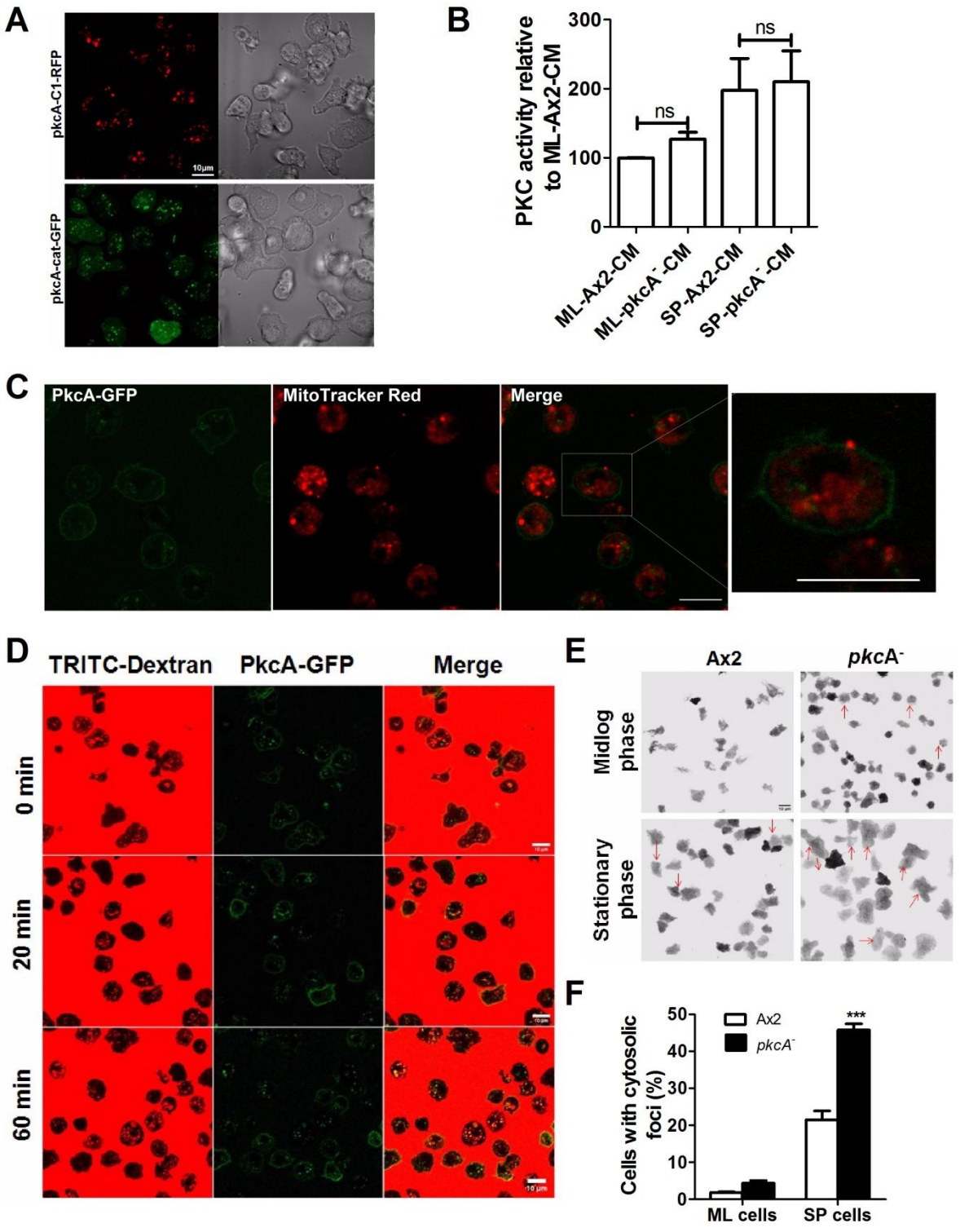

Fig. S7. PkcA-GFP localization in lysosomal vesicles and PkcA regulates lysosome dependent processes. (A) Representative images showing regulatory C1 domain (pkcA-C1-RFP) and catalytic kinase domain (pkcA-cat-GFP) localization in Ax2 cells. Scale bar -10µm. (B) A PKC activity assay was performed in ML and SP CM. The activity is normalized to ML-Ax2-CM. Data are means ± SEM; n=3 biologically independent samples. Statistical significance was determined using a one tailed paired *t*-test. ns-not significant. (C) PkcA-GFP containing cells were treated with MitoTracker Red and visualized by confocal microscope. Scale bar -10µm. (D) PkcA-GFP containing cells were incubated with 2mg/ml TRITC-dextran and imaged at the indicated time points. Scale bar -10µm. Scale bar- 10µm. (E and F) *PkcA*$^{-}$ cells have higher protein aggregation. Image of GFP spots (E) and Quantification of GFP spots (representing polyQ foci) (F). At least 50 cells were analyzed per experiment. Scale bar- 10µm. Data represents means ± SEM from n=3 independent experiments. In E, statistical significance was determined using a one tailed paired *t*-test. ***p<0.001.

Fig. S8. *PkcA* regulates *i6kA* expression levels.

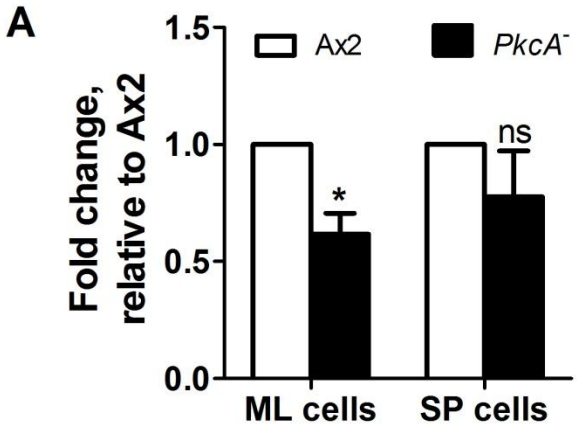

B

* x-[S/T]-x-[R/K]- Consensus PKC phosphorylation site

		Netphos 3.1 prediction score
9 S	YLVNSKKSK	0.860
572 S	PSNRSTRSN	0.864

Fig. S8. PkcA regulates *i6kA* expression levels. (A) qRT-PCR for *i6kA* gene expression in ML and SP cells. Data are means ± SEM; n=3 biologically independent samples. Statistical significance was assessed by one tailed paired *t*-test. *p<0.05 and ns-not significant. (B) Probable PKC phosphorylation sites in i6kA protein sequence determined using NetPhos 3.1.

Fig. S9. SDS-PAGE gel images used to quantify F-actin and Myosin levels.

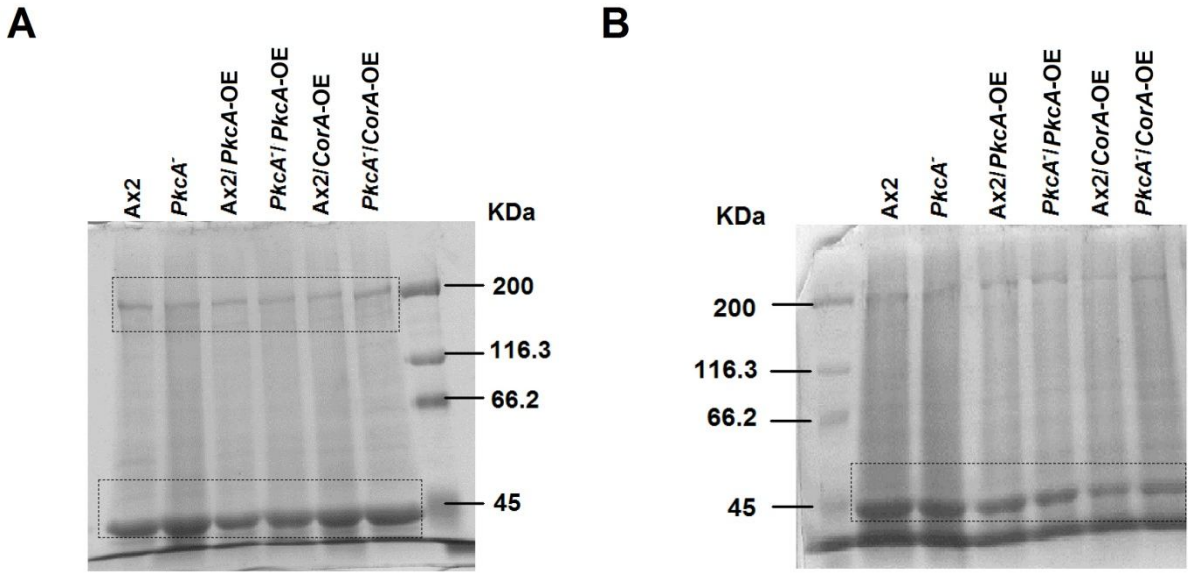

Fig. S9. SDS-PAGE images were used to quantify F-actin and myosin levels. Cytoskeletal fraction from cells grown in (A), shaking and (B), non-shaking conditions. The solid line box indicates assembled myosin bands and the dashed line box indicates F-actin bands. Refer Fig.6B,CD for F-actin quantification graph and Fig. S6B for myosin quantification graph

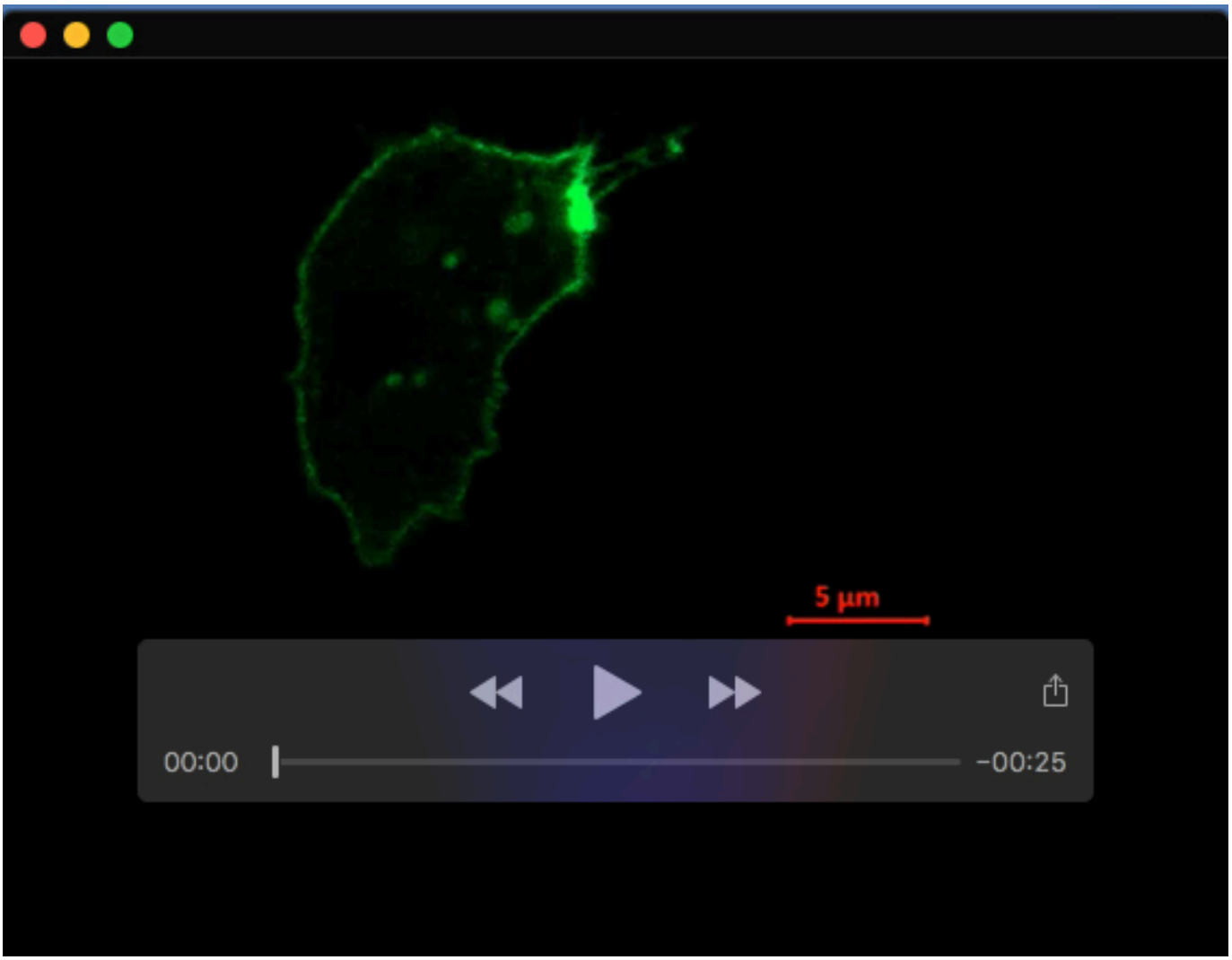

Movie 1. PkcA-GFP is localized to vesicles and the plasma membrane.

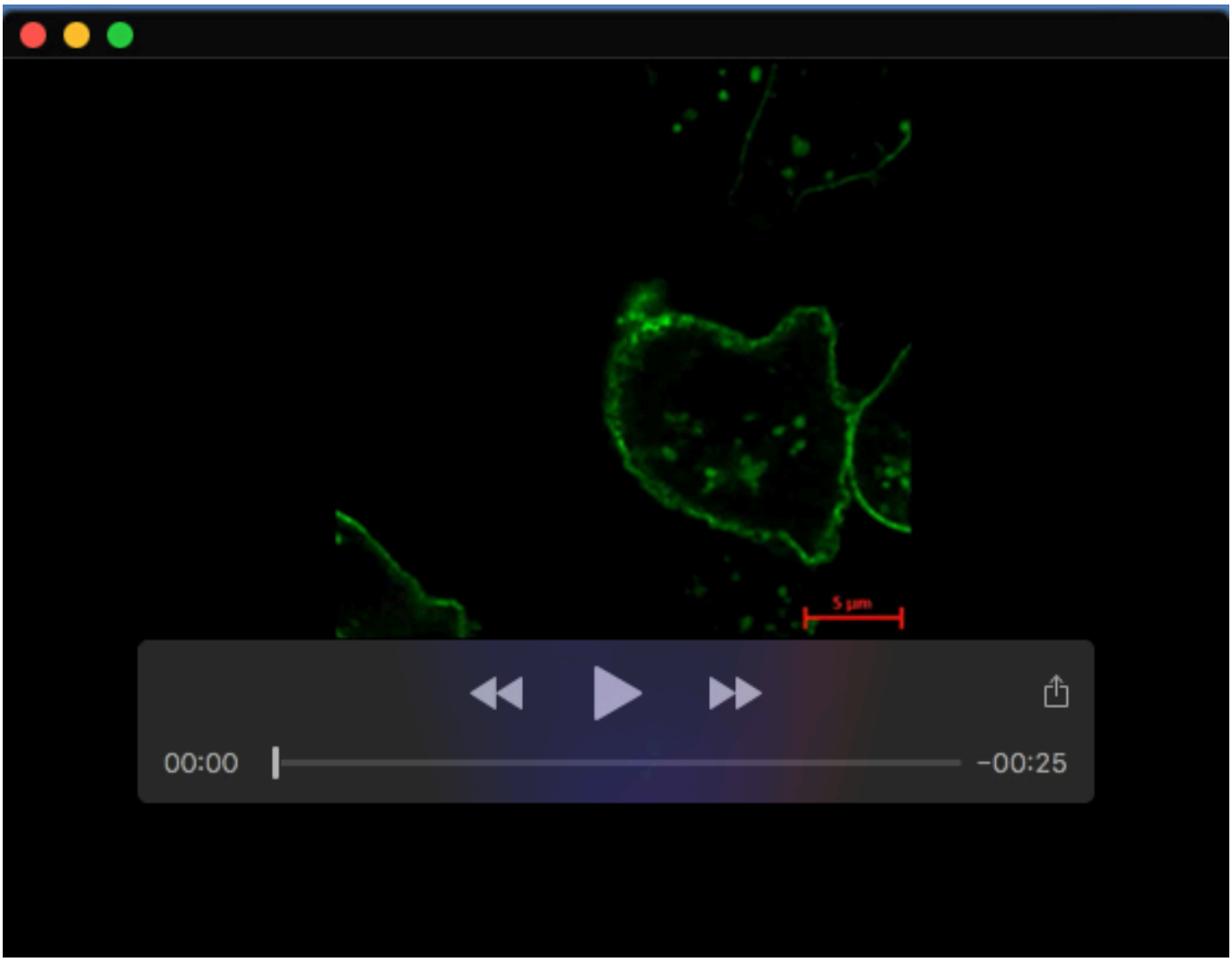

Movie 2. PkcA-GFP in motile cells. In motile cells, PkcA-GFP was accumulated to the rear end.

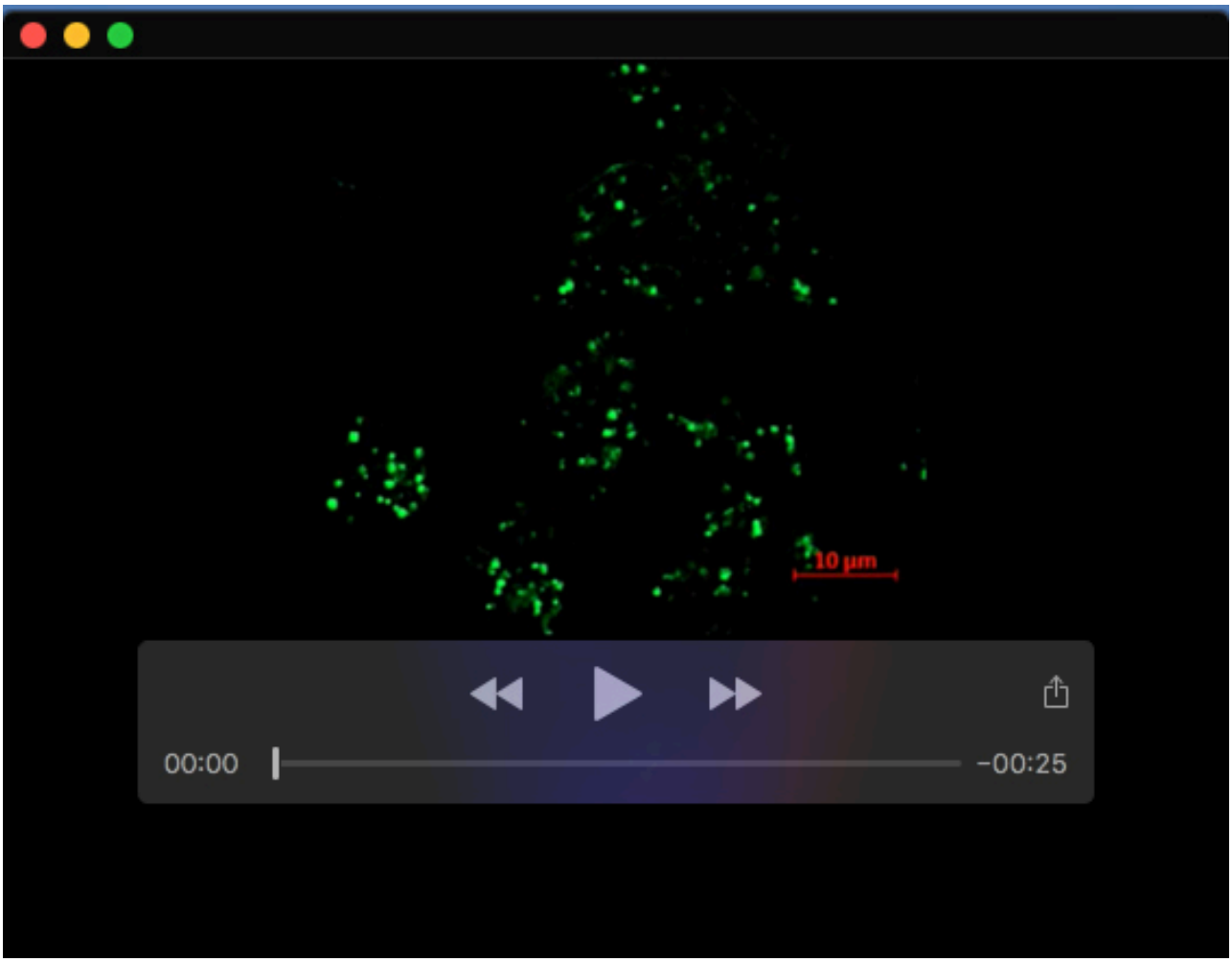

Movie 3. PkcA localization is not affected by DMSO (control)

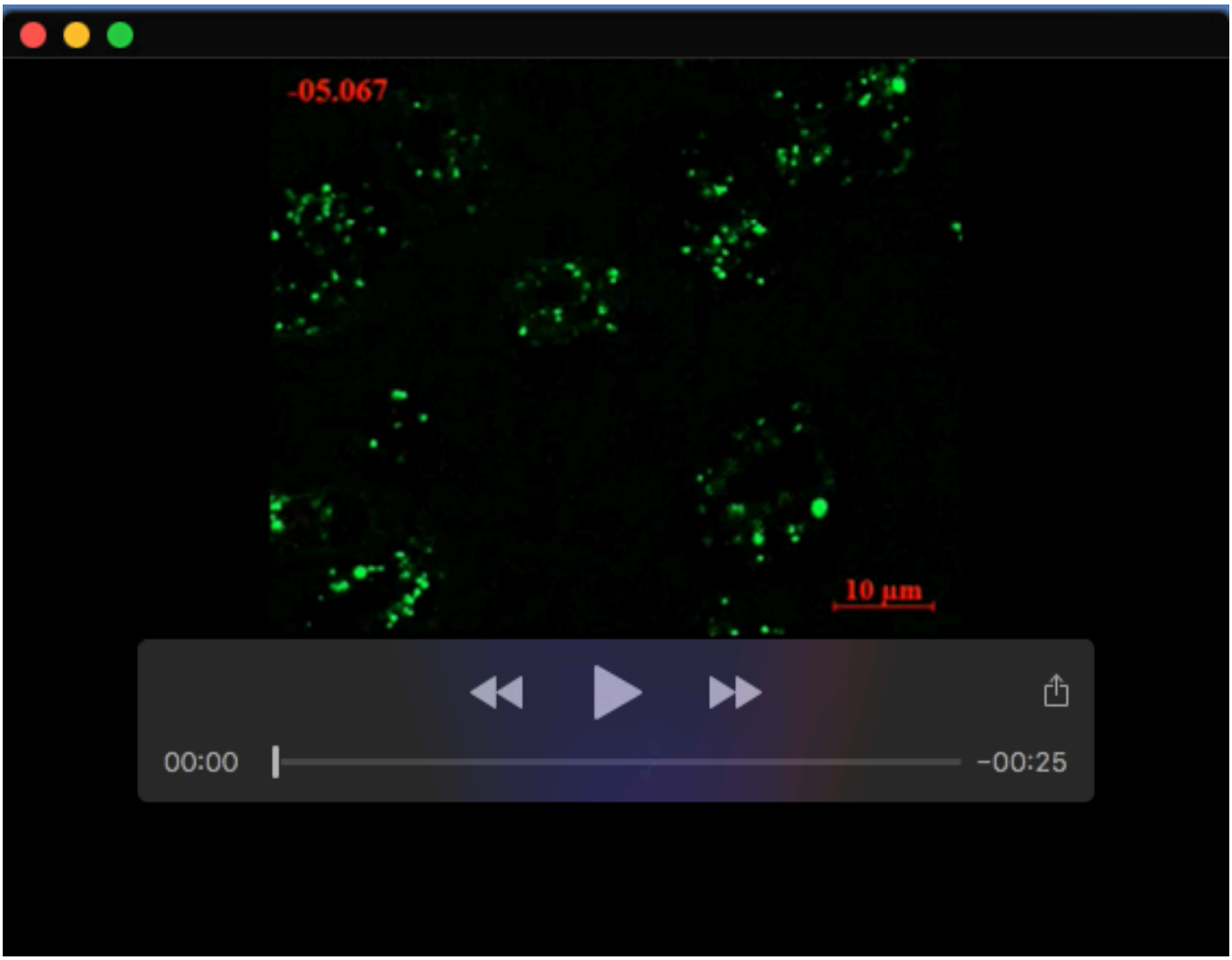

Movie 4. PkcA-GFP localization is not affected by PKC activity. To ascertain if the PKC activity is required for pkcA-GFP localization, Ax2/*act*15::*pkcA*-GFP cells were treated with 10 µM Bis I and pkcA-GFP localization was visualized.

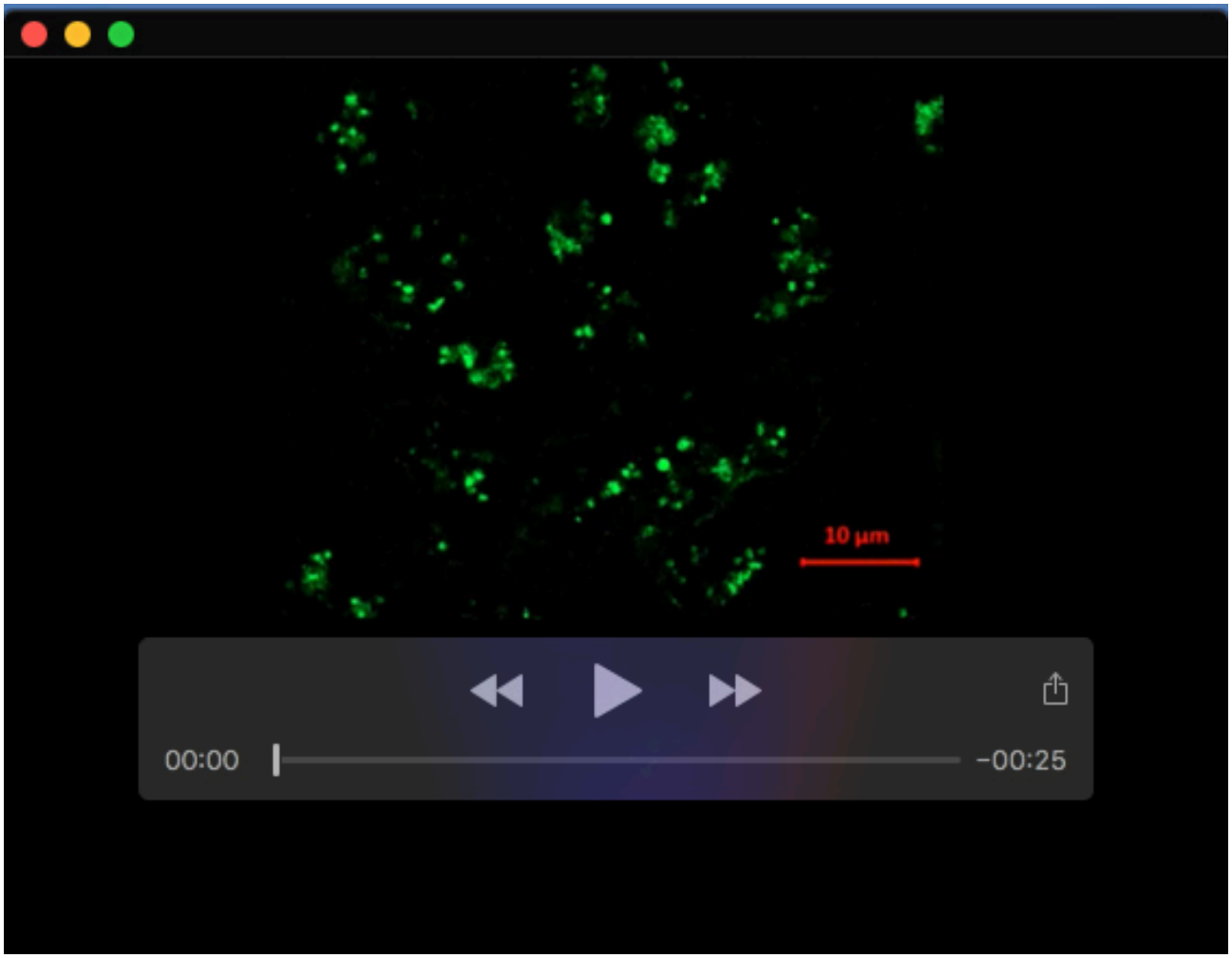

Movie 5. Actin polymerization is important for pkcA-GFP containing vesicular movement. To ascertain if actin polymerization is important for pkcA-GFP movement, Ax2/*act*15::*pkcA*-GFP cells were treated with 10 µM Latrunculin B and pkcA-GFP localization was visualized. Lat B treated cells round up and although the membrane localization of pkcA-GFP was intact, pkcA-GFP containing vesicles clutter together and showed no further movement. Thus, for vesicular pkcA-GFP localization actin polymerization is important.

Table S1. Stationary phase cell density in different conditions.

Conditions		Maximum observed cell density (× 10^6 cells/ml)	
		Ax2	***pkcA*⁻**
Growth assay[a]		25.1 ±1.2	12.6±0.4 ***
Growth of SP- *pkcA*⁻ cells in fresh HL5[b]	Initial SP cell density	22.6±1.1	13.8±0.6*
	In fresh HL5 (at the SP cell density)	44.8±2.4	24.2±2.5****
	In CM (at SP cell density)	20.1±4.0	6.9±1.8****
	In fresh HL5 (at ¼ th of SP cell density)	23.1±1.1	13.4±0.7**
	In CM (at ¼ th of SP cell density)	6.2±0.9	4.5±0.6^{ns}
Initial cell density[b]	1×10^5 cells/ml	20.4±1.2	13.6±0.8***
	5×10^5 cells/ml	17.9±1.2	10.6±1.0**
	1×10^6 cells/ml	18.7±1.8	13.8±0.9*
Rotation speed[b]	50 rpm	4.8±0.3	5.2±0.9^{ns}
	100 rpm	14.2±1.4	10.3±0.4**
	150 rpm	19.9±0.7	12.0±0.6****
Flask size[b]	25ml	18.5±0.8	12.7±1.0*
	50ml	22.0±1.4	14.2±0.2**
	100ml	20.0±1.8	12.6±2.5**
ScPPX1 treatment[b]	Control	19.6±2.3	14.0±0.4*
	0.15µg/ml ScPPX1	37.5±2.0	24.8±2.9**
CorA overexpression[b]	Controls	25.2±0.8	13.9±0.4***
	CorA-OE	23.8±1.53	22.30±1.04^{ns}
Different concentrations of HL5 media[b]	0.5X	4.0±0.5	3.3±0.7^{ns}
	1X	21.8±1.2	13.8±0.3**
	2X	26.4±2.2	23.0±2.5^{ns}

SP cell density upon Bis I treatment[a]**.**	
Bis I treatment	**Maximum observed cell density, ×10^6 cells/ml**
Ax2	21.4±0.6
pkcA⁻	12.7±0.4***
Ax2 + 1 µM Bis I	17.1±0.6***,###
Ax2 + 3 µM Bis I	17.5±0.7***,###
Ax2 + 5 µM Bis I	14.1±0.6***,ns
Ax2 + 10 µM Bis I	11.9±0.8***,ns
Ax2 + 20 µM Bis I	10.1±0.6***,ns
Ax2 + 40 µM Bis I	10.4±0.3***,ns
pkcA⁻ + 5 µM Bis I	12.4±0.1^{ns}
pkcA⁻ + 10 µM Bis I	11.1±0.5$^{\#}$
pkcA⁻ + 20 µM Bis I	10.9±0.2$^{\#\#}$
pkcA⁻ + 40 µM Bis I	10.3±0.3$^{\#\#\#}$
SP cell density of strains carrying individual domains of pkcA[a]**.**

Cell type	Maximum observed cell density, $\times 10^6$ cells/ml
Ax2	25.0±0.2
pkcA$^-$	10.8±1.6***
pkcA$^-$/ *pkcA*-C1	10.8±0.6***
pkcA$^-$/ *pkcA*-Cat	10.8±1.3***
pkcA$^-$/*pkcA*-OE	18.6±2.1^{ns}

[a]one- way ANOVA with Tukey's multiple comparisons
[b]two-way ANOVA with Bonferroni's multiple comparisons
Comparison with Ax2 are represented as ****p<0.0001,***p<0.001,**p<0.01, *p<0.05. and ns-not significant. Comparison with *pkcA*$^-$ are represented as $^{###}$ p<0.001, ,$^{##}$p<0.01, $^{#}$p<0.05. and ns-not significant.

Table S2. SP cell density and polyP levels in pinocytosis and exocytosis defective mutants

Cell type	Maximum observed cell density, $\times 10^6$ cells/ml	PolyP levels /10^6 cells
Ax2	20.8±0.9	9.6±0.4
PkcA$^-$	3.9±0.2[a]	60.9±1.3[b]
AbpA$^-$/*C*$^-$	5.9±1.0[b]	37.8±4.9[a]
ProA$^-$/*proB*$^-$	14.2±0.8[b]	1.6±0.1[b]
NC4A2	14.8± 0.4	14.7±1.7
LvsB$^-$	3.8±0.4[c]	83.5±8.3[d]
HPS400	13.8 ±0.8	14.9 ± 0.8
ScarA$^-$	0.2 ±0.02[e]	736.7 ± 54.3[e]

[a] $p<0.01$ compared with Ax2(two-tailed paired *t*-test).
[b] $p<0.0001$ compared with Ax2(two-tailed paired *t*-test).
[c] $p<0.0001$ compared with NC4A2 (two-tailed paired *t*-test).
[d] $p<0.001$compared with NC4A2 (two-tailed paired *t*-test).
[e] $p<0.0001$ compared with HPS400(two-tailed paired *t*-test).